

New Adaptive Algorithm for Power Efficiency in VLC Links

V. Guerra¹, J. Rabadan¹, J. Rufo², R. Perez-Jimenez¹

¹IDeTIC- ULPGC, PCT Tafira, Edif. Polivalente II, 35017 Las Palmas, Spain

²Lightbee S.L., PCT Tafira, Edif. Polivalente III, 35017 Las Palmas, Spain

{vguerra; jrabadan, rperez}@idetec.eu; jrufu@lightbeecorp.com

Abstract- Power control algorithms are a well-known strategy to optimize SNR in highly interfered environments. Furthermore, sensor nodes, which are battery-powered, have expensive replacement costs. Hence, strategies to reduce the power consumption are mandatory in this kind of device, and power control algorithms can be energy-optimized. In this paper, a new power control, Adaptive-Step-and-Damping algorithm - ASDA- is presented. It enhances the resulting energy efficiency compared with the classic Newton-Raphson gradient-descent algorithm (equivalent to an LMS algorithm)

Keywords-Energy efficiency. Power Control Algorithm. VLC isolated nodes

I. INTRODUCTION

Energy efficiency is one of the most important aspects of VLC sensor networks [1-3]. The power consumption of battery-powered isolated nodes defines their lifespan, and taking into account the high replacement costs, it is a primary minimization objective. The power consumption of a node is usually defined as a sum of partial contributions: The main consumptions are related to processing (CPU and control), communication interfaces and payload. This last aspect can widely vary depending on the purpose of the deployed node. For monitoring applications, the payload comprises sensors and acquisition circuitry, which can normally be neglected respect to communications. However, for applications where actuation is needed, the payload power consumption may be the primary source of energy usage.

Energy efficiency can be improved in different manners. Using a layered approach, the best options to enhance the efficiency are the physical and the medium access layer. Regarding the VLC physical layer, modulations and encoding with pulsed shapes are normally better alternatives than continuous waveforms such as OFDM or CSK [4]. However, these types of signals can be Pulse Width Modulated to take advantage of high efficiency nonlinear drivers [5]. Therefore, between PHY and MAC layers, power control algorithms are an interesting option to adopt the emitted power of the isolated nodes and hence, reduce the power consumption.

Power control is the selection of the transmission output power in a communications system, attending to an optimization criterion. This criterion is normally a combination of energy minimization and the satisfaction of a minimum performance on the receiver. Traditionally, PCAs have been used to maximize the SNR while keeping the overall interference below a threshold in wireless communication channels, such as UMTS [6]. In this case, since all the signals are transmitted at the same time, each one spread by its corresponding orthogonal code, if there is no power control, the interference level may increase up to harmful levels, dramatically reducing the BER. In the case of VLC, PCAs are not proposed as SNR-improving techniques, but as energy-saving algorithms. BER is important since it partially defines the number of packet retransmissions, which is very power consuming. However, the possibility to adapt the transmission power to an optimum value, regarding energy, has more weight in the design of isolated optical nodes. Almost any energy-saving protocol or technique is justified in isolated sensor networks because the extension of the nodes' lifespan dramatically reduces the replacement costs.

In this work, a new adaptive-step algorithm, which reduces the dependence of the channel's variability knowledge it proposed. It introduces an adaptive-damping version of that algorithm, where the damping factor is automatically adapted.

Next sections are organized as follows. Section 2 compares different PCA and explains the changes introduced in the proposed algorithm. In Section 3 we present the results corresponding to the application of different PCA to variable VLC scenarios and demonstrate the advantages of the proposed scheme. Finally, in section 4, the work conclusions are discussed.

II. POWER CONTROL ALGORITHMS

There are different taxonomies of power control algorithms, depending on the classification criterion. For instance, if each node takes its own decisions the algorithm is distributed while on the other case is centralized. If there is channel status exchange between nodes, ergo, there is information feedback, the algorithm is closed-loop. On the contrary, it is open-loop. Finally, depending on how is

calculated the step size of the iterative power control process, the algorithms can be fixed-step, variable-step or adaptive-step.

In this work, a VLC access point with a mobile user whose channel response is affected by a random pointing angle or by a random walk behavior is considered. Figure 1 represents the studied scenario, which comprises a main energy-unlimited node and a mobile battery-powered remote node.

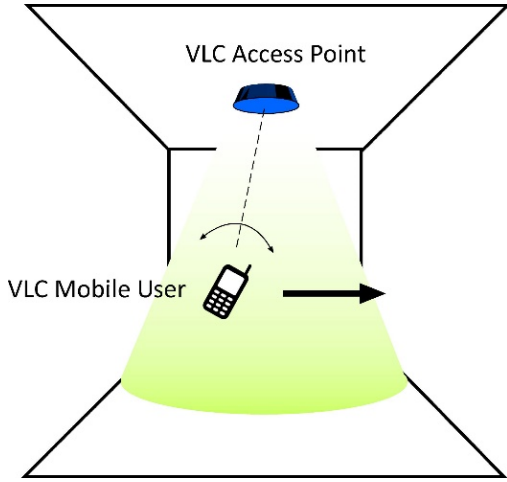


Figure 1: Scenario under consideration to study power control algorithms

Additionally, the studied algorithms are centralized and closed-loop. The centralization of the algorithms has been proposed to reduce the remote node's complexity. Furthermore, the estimation of the link's performance takes place at the main node's side while the uplink (main node to remote node) is always carried out at maximum power. The feedback of channel information is necessary to estimate with a lower error the needed transmit output power, but it also adds an error source that should be taken into account. A power control algorithm is derived from an optimization problem of the type defined in equation 1:

$$\min \sum_i P_i \quad (1)$$

Subject to:

$$\frac{(P_i g_{ii})^2}{\sigma_N^2 + 2qB \sum_j P_j g_{ij} + \sum_{j \neq i} (P_j g_{ij})^2} \geq K_i \quad (2)$$

σ_N^2 is the sum of the receiver's inherent noise powers and K_i is the SINR threshold for the i -th channel. g_{ij} is the channel gain, including the responsivity, between the i -th receiver and the j -th emitter. Note that the quadratic term of the denominator is the optical interference term, while the linear term is the sum of all the shot noises due to both interferences and wanted signals. These last two terms are

nullified in the proposed scenario, due to the orthogonality of each channel after the use of a TDMA scheme, yielding the following simplified version of the convex minimization problem (Equations 3 and 4).

$$\min \sum_i P_i \quad (3)$$

Subject to:

$$\frac{(P \cdot g)^2}{\sigma_N^2 + 2qBP \cdot g} \geq K \quad (4)$$

The power is usually minimized iteratively, as shows Equation 5

$$P^{(i+1)} = P^{(i)} + \Delta P^{(i)} \quad (5)$$

$P^{(i+1)}$ is the next transmission power and $\Delta P^{(i)}$ is the calculated step. Depending on how this step is calculated, the algorithm would be fixed-step, variable-step or adaptive-step. Other important aspect of the algorithms is how the SNR condition is estimated. The most common strategies are the following:

- BER: it is directly related to the SNR through the complementary error function. As the modulation or encoding spectral efficiency increases, the BER becomes more sensitive to the SNR. The main disadvantage of this indirect estimation is the requirement of long integration periods to retrieve a sufficient amount of data to perform the calculation.
- Direct SNR estimation. The SNR is the ratio between the squared expected value and the variance of a signal. This estimation needs a high number of samples to present a reliable confidence interval. However, if a soft signal detection were performed using a DSP or a FPGA, this estimation could be real-time performed.
- Received power estimation. For situations in which the shot noise could be neglected, the SNR condition can be directly calculated using Equation 4. Furthermore, this technique is suitable for low-power devices, since only a few number of samples per frame are needed. Low pass filtering may be used to reduce noise before sampling, or a few samples from a long-duration synchronization header could be acquired to estimate the received power.

$$(P \cdot g)^2 \geq K \cdot \sigma_N^2$$

$$(P \cdot g) \geq K^{1/2} \cdot \sigma_N \quad (6)$$

Some of the proposed centralized algorithms need knowledge of the remote node's emission parameters: energy efficiency, allowed power codes, transimpedance conversion factor, etcetera. Therefore, an initialization stage to retrieve the necessary information is needed before the execution of the PCA. Figure 2 depicts the stages of the proposed PCAs.

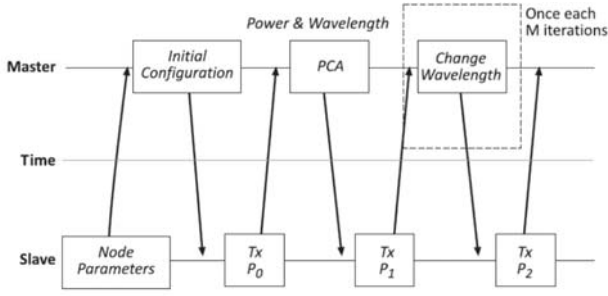


Figure 2: Sequence of the proposed UWOC power control algorithms

a. Fixed-step algorithm

Fixed-step algorithms are the easiest approach to energy minimization. Depending on the result of Equation 7, the output power is incremented $N\delta$ or decremented $M\delta$. Mathematically:

$$P^{(i+1)} = P^{(i)} + \Delta P^{(i)}$$

$$\Delta P^{(i)} = \begin{cases} N\delta & (P \cdot g) < K^{1/2} \cdot \sigma_N \\ -M\delta & (P \cdot g) \geq K^{1/2} \cdot \sigma_N \end{cases} \quad (7)$$

This algorithm is characterized by its low convergence speed and its low stability after reaching the optimum value. However, it is very memory and computationally-efficient.

b. Variable-step algorithm

Variable step algorithms are the logical evolution of fixed step algorithms to improve the speed. In this case, the step is gradually incremented on the direction defined by Equation 8. Mathematically:

$$P^{(i+1)} = P^{(i)} + \Delta P^{(i)}$$

$$\Delta P^i = (\alpha_i - \beta_i) \cdot \delta \quad (8)$$

$$\alpha_i = 0; \beta_i = \beta_{i+1} + 1 \quad (P \cdot g) < K^{1/2} \cdot \sigma_N$$

$$\alpha_i = \alpha_{i+1} + 1; \beta_i = 0 \quad (P \cdot g) \geq K^{1/2} \cdot \sigma_N$$

This algorithm presents a higher convergence speed respect to fixed-step, but also a higher recovery speed after a channel loss. However, the stability after convergence is worse in this case. Fixed-step algorithms operate without memory, but variable-step algorithms need to store a one-sample history.

c. Adaptive-step algorithm

Adaptive-step algorithms modify the power correction step $\Delta P^{(i)}$ at each iteration, depending on the received power and the distance to the optimum value. In order to obtain an adaptive method, a gradient descent strategy can be applied to Equation 6. For instance, a Newton-Raphson method may be used, defining an optimization function $F(P) = 0$ after the mentioned condition, yielding:

$$P^{(i+1)} = P^{(i)} + \Delta P^{(i)}$$

$$\Delta P^{(i)} = -\alpha \frac{F(P^{(i)})}{\left. \frac{\delta F(P)}{\delta P} \right|_{P=P^i}} \quad (9)$$

α is a relaxation coefficient to smooth the convergence of the output power. From the optimization restriction, and naming $K_0 = K^{1/2} \sigma_N$, it can be demonstrated that:

$$\Delta P^{(i)} = -\alpha \frac{P^{(i)} g^i - K_0}{g^{(i)}} \quad (10)$$

Introducing Equation 9 in Equation 10, it yields the final form of the adaptive-step algorithm. Note that $g^{(i)}$ is the estimated channel gain at each iteration, this gain depends on the variability of the channel and it defines the after-convergence variability of the algorithm.

$$P^{(i+1)} = (1 - \alpha)P^{(i)} + \alpha \frac{K_0}{g^{(i)}} \quad (11)$$

The resulting algorithm presents the same form as a LMS algorithm. Furthermore, it can be observed that this algorithm needs the estimation of the channel gain. Introducing an output power code in the header of the transmitted frame, the receiver would be able to estimate the channel gain according to the measured received power. However, this procedure introduces an extra error source, since low SNR situations could generate bit errors and hence, unrealistic channel gains. The convergence speed is the best in this algorithm, whilst the after-convergence variability depends on the channel gain estimations. However, to ensure that this algorithm converges, the damping factor must be bounded. Extending the iterative equation of the output power from $i = 0$ to $i = n + 1$ it yields:

$$P^{(n+1)} = (1 - \alpha)^{n+1} P^{(0)} + \alpha K_0 \sum_{j=0}^n \frac{(1-\alpha)^j}{g^{(n-j)}} \quad (12)$$

This last summation needs to be converging to ensure the stability. The simplest weak condition is to force each term to be smaller than the previous one. Mathematically:

$$\alpha g^{(i)} > |g^{(i+1)} - g^{(i)}| \quad (13)$$

It must be taken into account that $g^{(i)}$ is a random process that describes the behavior of the channel gain at uncorrelated instants. Intuitively, α can be adapted to the channel's random nature regarding the expected value of the last equation, yielding:

$$E[\alpha] > \frac{E[|g^{i+1} - g^i|]}{E[g^i]} \quad (14)$$

It can be observed that from Equation 14, α must be in the interval (0, 1). Furthermore, both convergence speed and variability depend on α . Large values of α filter the output power and reduce the convergence time. On the other side, small values increment the variability and reduce the convergence speed. The following algorithm tries to obtain a compromise solution on both parameters.

d/ Adaptive-Step-and-Damping algorithm

The last subsection introduced adaptive-step algorithms, but the convergence needs a high knowledge of the channel's variability. Regarding the observed variability of the VLC

channel and the wide range of phenomena that may occur, an adaptive-damping version of the last algorithm is proposed. This algorithm adapts the damping factor α automatically. Analyzing Equation 14, it can be noticed that it expresses the variability of the channel. Hence, to reduce the variability of the algorithm, α can be iteratively modified with a parameter modeling this variability. Equation 15 shows the iterative formula.

$$\alpha^{(i+1)} = \frac{\alpha^{(i)} + \xi^i}{2}; \xi^i = \frac{2\sigma_i}{\mu_i + \sigma_i} \quad (15)$$

μ and σ are the mean and standard deviation of the channel gain. ξ is the estimation of the channel's variability, where σ is always lower than μ due to the nature of the VLC channel. The final value of $\alpha^{(i)}$ is then averaged with the estimated variability to obtain the next iteration value.

III. SIMULATION RESULTS

In this section, several simulation results for different scenarios are obtained. In order to test the robustness of the algorithms, scenarios with different variabilities have been tested (Table 1). The emitter has a minimum output power of 10 mW and a maximum of 10 W, encoded in 8 bits.

Scenario	μ	σ	ξ
1	10^{-3}	10^{-4}	0.2
2	$2.5 \cdot 10^{-3}$	10^{-5}	0.3
3	10^{-5}	10^{-6}	0.4

Table 1. Parameters of each simulated scenario

Two main statistics are obtained to describe the performance of each algorithm: convergence iteration (CI) and after-convergence variability (ACV). The convergence iteration is defined as the iteration at which the output power is below $1.1P^{(\infty)}$. The after-convergence variability is the variance of the output power after the convergence iteration. The following figures depict the behavior of the presented algorithms at each scenario. For simulation purposes $K_0 = 10^{-5}$. Table 2 summarizes the obtained statistics for each scenario and algorithm on the form (CI/ACV). Figures 3, 4 and 5 show the evolution of the output power calculated by the different implemented PCAs (Fixed Step, Variable Step Adaptive Step [0.25], Adaptive Step [0.75] and Adaptive-Damping), for the three proposed scenarios.

Scenario	1	2	3
FS	$(101/3.13) \cdot 10^{-4}$	107/0.016	45/0.05
VS	46/0.001	55/0.1	30/0.024
AS ($\alpha=0.25$)	$(24/8) \cdot 10^{-7}$	59/0.115	9/0.103
AS ($\alpha=1$)	$(6/3.13) \cdot 10^{-6}$	6/0.48	4/0.445
ADSA	$2 \cdot 10^{-13}$	2/0.0026	$(2/9.6) \cdot 10^{-4}$

Table 2: Simulations results summary

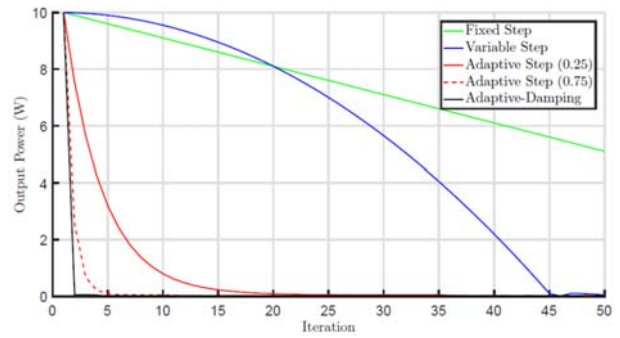


Figure 3: Evolution of the output power for Scenario #1

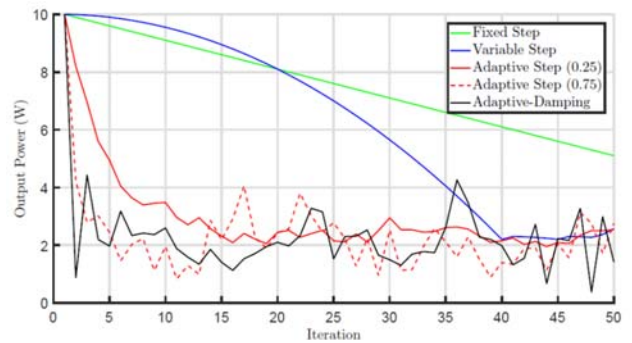


Figure 4: Evolution of the output power for Scenario #2

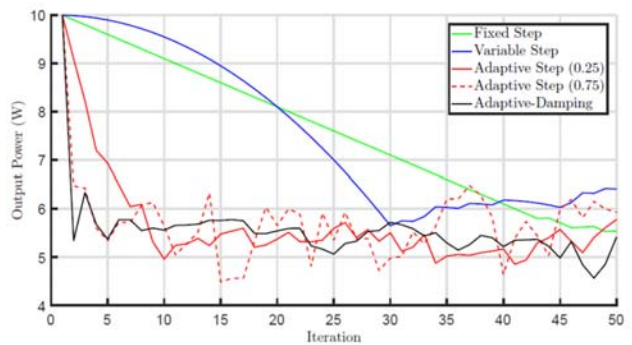


Figure 5: Evolution of the output power for Scenario #3

It can be observed that Fixed-Step and Variable-Step algorithms present a reduced variability, however, their convergence iteration is several times greater than the adaptive algorithms. Regarding Adaptive-Step, the results suggest that the compromise between variability and speed is highly dependent on α . This dependency is eliminated using the Adaptive-Step-and-Damping algorithm. In addition, very low values of α may need a huge amount of samples to recover from a change in the mean channel gain (an increasing or decreasing link range in AP-to-node communication for instance). The proposed algorithm presents the lowest variability although the calculation of the variability parameter was performed using only 5 samples.

a. Influence of the stored history size

The Adaptive-Step-and-Damping algorithm needs to store a certain amount of channel gain samples in order to calculate the damping factor according to Equation 15. Due to the variability of the channel, the calculated value of α is subject to a correct estimation of both μ and σ . The used estimators are shown in Equations 16 and 17.

$$\mu = \frac{1}{N} \sum_{j=1}^N g^{(i)} \quad (16)$$

$$\sigma = \sqrt{\frac{1}{N} \sum_{j=1}^N (g^{(i)})^2 - \mu^2} \quad (17)$$

From a simple statistical analysis and assuming normality on the distribution (which is an obvious error), it can be shown that:

$$\mu \approx N \left(E[g], \frac{1}{N} Var(g) \right) \quad (18)$$

$$\sigma \approx NC - \chi_N(E[g], Var(g)) \quad (19)$$

The sample mean follows approximately a normal distribution whose variance is directly reduced by the number of samples, whilst the standard deviation follows a noncentral χ distribution with N degrees of freedom. The variance of a noncentral χ distribution also decreases with the number of samples. Rearranging the terms of Equation 13, it can be shown that α follows a distribution which is related to the reciprocal of the ratio μ/σ . Therefore, the expected value of α can be approximated by:

$$E[\alpha] < \frac{2}{1+E[\mu]/E[\sigma]} \quad (20)$$

Obviously, an error is being committed due to the nonzero correlation between mean and standard deviation. However, empirical observations of the correlation coefficients between the two variables suggest that the higher the degrees of freedom, the lower the correlation. Due to the elevated number of samples needed to accurately estimate the variance of σ , the variability of α is very sensitive to the actual variability of the channel. This aspect of the algorithm should be further investigated to make it more robust. Figure 6 shows the values of $E[\alpha]$ and $Var(\alpha)$ for different history sizes.

The values were obtained for Scenario #2, which is the more variable of the three studied. The actual variability parameter (Equation 13) at which α is associated was 0.8213. It can be observed that the higher the History Size, the better is estimated the variability of the channel. However, as the History Size increases, the delay between abrupt changes on the channel gain and the response increases.

b. Complexity comparison between algorithms

The complexity of the power control algorithm may be of capital importance for application with limited memory and computation resources. The presented memory complexity is presented in terms of the needed history size, whilst the computational complexity is detailed in sums, products and

more complex operations (power, square root, division, etc...). Table 3 summarizes the complexities.

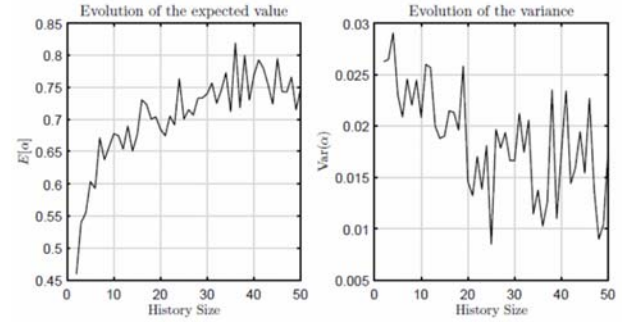


Figure 6: Relationship between the expected value of (left) and its variance (right) with the History Size

Algorithm	Memory	Sums	Products	Other operations
Fixed-Steps	0	1	1	0
Variable-Step	0	2	1	0
Adaptive-Step	1	1	2	1
Adaptive-Step-and-Damping	N	2N+3	N+4	2

Table 3: Memory and computation complexities of the presented PCAs

The number of operations in the ASDA algorithm increases linearly with N using an inefficient calculation of the mean value and the standard deviation where, at each iteration, the whole stored array is swept. However, there are more efficient implementations that may reduce the complexity to $O(\log N)$. Furthermore, depending on the number of remote nodes handled within the TDMA scheme, the memory requirements may turn this algorithm not feasible. In that case, the history size should be decreased. Figure 7 depicts an example of the behavior of the output power (for the scenario #2 case).

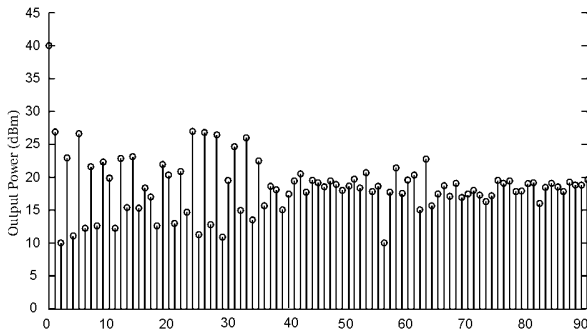


Figure 7: Output power using the ASDA algorithm

The energy saving \mathcal{E} of the PCA can be calculated as:

$$\mathcal{E} = 1 - \frac{1}{\eta_{min} P_{max}} \lim_{n \rightarrow \infty} \frac{1}{N} \sum_{i=1}^N \eta(\lambda_i) P^{(i)} \quad (21)$$

Using this equation, it can be observed that the sole fact of including a PCA such as the ASDA algorithm, produces an energy saving in the communications interface of a 50.47 %.

IV. CONCLUSIONS

In this work, a new PCA algorithm has been proposed in order to improve the energy-efficient strategies to reduce the power consumption of battery-powered nodes. Power control algorithms dramatically reduce the power consumption. Traditionally, power control has been used in cellular networks to maximize the SINR, controlling the output power to generate the lowest possible interference. However, in VLC sensor networks the main objective is to reduce the power consumption as much as possible, due to the elevated replacement costs. Several power control algorithms were tested under simulated conditions, and an Adaptive-Step-And-Damping power control algorithm was proposed to enhance the convergence time and reduce the variability of the output power. It was proven that this modification of the LMS algorithm can dramatically improve the energy efficiency respect to a constant power scheme adding very small complexity.

ACKNOWLEDGMENTS

This work was supported in part by the Spanish Research Administration (MINECO, OSCAR Research Program)

REFERENCES

- [1] V. Guera-Yanez Contribution on the study of Underwater Wireless Optical links: Channel estimation and energy efficiency. PhD Thesis at ULPGC. Apr. 2016
- [2] Rufo, J., et al. "Considerations on modulations and protocols suitable for visible light communications (VLC) channels: Low and medium baud rate indoor visible lighth communications links." Consumer Communications and Networking Conference (CCNC), 2011 IEEE. IEEE, 2011.
- [3] Perez-Jimenez, R., et al. "Visible light communication systems for passenger in-flight data networking." Consumer Electronics (ICCE), 2011 IEEE International Conference on. IEEE, 2011
- [4] Luna-Rivera, J. M., Perez-Jimenez, R., Guerra-Yanez, V., Suarez-Rodriguez, C., & Delgado-Rajo, F. A. (2014). Combined CSK and pulse position modulation scheme for indoor visible light communications. *Electronics Letters*, 50(10), 762-764.
- [5] del Campo-Jimenez, G., Perez-Jimenez, R., & Lopez-Hernandez, F. J. (2016). Constraints on drivers for visible light communications emitters based on energy efficiency. *Optics express*, 24(9), 9994-9999.
- [6] "Umts definition"
<http://www.3gpp.org/technologies/keywords-acronyms/103-umts>. 3GPP website. Tavel, P. 2007
 Modeling and Simulation Design. AK Peters Ltd.